# Speeding up the antidynamical Casimir effect with nonstationary qutrits

A. V. Dodonov,[1,*] J. J. Díaz-Guevara,[2] A. Napoli,[3,4] and B. Militello[3,4]

[1]*Institute of Physics and International Centre for Condensed Matter Physics, University of Brasilia, 70910-900, Brasilia, Federal District, Brazil*

[2]*Departamento de Física, Universidad de Guadalajara, Revolución 1500, Guadalajara, Jalisco 44420, Mexico*

[3]*Dipartimento di Fisica e Chimica, Università degli Studi di Palermo, Via Archirafi 36, I-90123 Palermo, Italy*

[4]*I.N.F.N. Sezione di Catania, via Santa Sofia 64, I-95123 Catania, Italy*

(Received 26 July 2017; published 12 September 2017)

The antidynamical Casimir effect (ADCE) is a term coined to designate the coherent annihilation of excitations due to resonant external perturbation of system parameters, allowing for extraction of quantum work from nonvacuum states of some field. Originally proposed for a two-level atom (qubit) coupled to a single-cavity mode in the context of the nonstationary quantum Rabi model, it suffered from a very low transition rate and correspondingly narrow resonance linewidth. In this paper we show analytically and numerically that the ADCE rate can be increased by at least one order of magnitude by replacing the qubit by an artificial three-level atom (qutrit) in a properly chosen configuration. For the cavity thermal state we demonstrate that the dynamics of the average photon number and atomic excitation is completely different from the qubit's case, while the behavior of the total number of excitations is qualitatively similar yet significantly faster.

DOI: 10.1103/PhysRevA.96.032509

## I. INTRODUCTION

The broad term *dynamical Casimir effect* (DCE) refers to the generation of excitations of some field (electromagnetic, in the majority of cases) due to time-dependent boundary conditions, such as changes in the geometry or material properties of the system [1–4] (see [5,6] for reviews; see also [7–9] for the related problem of a particle in a wall with moving boundaries). In the so called *cavity DCE* one considers nonadiabatic (periodic or not) modulation of the cavity natural frequency by an external agent, investigating the accumulation of intracavity photons or the photon emission outside the cavity [1,10–12]. The additional interaction of the cavity field with a stationary "detector" during the modulation (harmonic oscillator, few-level atom, or a set of two-level atoms in the simplest examples) may dramatically alter the photon generation dynamics, for instance, altering the field statistics, shifting the resonance frequency, and inhibiting the photon growth [13–19] (see [20] for a short review). Moreover, the degree of excitation of the detector varies according to the regime of parameters, and entanglement can be created between the cavity field and the detector, or between the atoms coupled to the field [21–25].

Over the past ten years a new path has attracted attention of the community working on nonstationary phenomena in cavity quantum electrodynamics (QED). Instead of changing the cavity frequency, different studies suggested the parametric modulation of the "detector" instead, promoting it from a passive to an active agent responsible for both the generation and detection of photons [26–35]. Besides eliminating the inconvenience of time-dependent Fock states of the field associated with time-varying cavity frequency [10], this scheme makes full use of the counter-rotating terms in the light-matter interaction Hamiltonian and does not require the inclusion of additional parametric down-conversion terms in the formalism [26,31,34,35]. Moreover, it benefits from recent advances in the coherent control and readout of microscopic few-level quantum devices developed in the realm of the circuit QED for applications in quantum information processing (see [36] for a recent review).

The area of circuit QED investigates the interaction of artificial superconducting atoms, formed by a sophisticated array of Josephson junctions, and the electromagnetic field confined in increasingly complex microwave resonators, ranging from waveguide resonators or 3D cavities [37–41]. The advances in engineering allowed for implementation of multilevel atoms, with controllable transition frequencies and coupling strengths, that can interact with multiple cavities and other atoms controlled independently [32,36,38,42–48]. Moreover, circuit QED allows for unprecedented atom-field coupling strength, in what became known as the ultrastrong and deep strong coupling regimes [49–52]. In the context of DCE, the exquisite control over the parameters of the Hamiltonian allows for multitone multi-parameter modulations [26,53–55], while quantum optimal control strategies can be used to enhance the desired effects [56].

Photon generation is not the only phenomenon induced by parametric modulations in circuit QED. It was shown recently that the counter-rotating terms can also be employed to annihilate excitations of the electromagnetic field from nonvacuum initial states, in what became known as the *antidynamical Casimir effect* (ADCE) [34]. This effect was predicted in the context of the quantum Rabi model, which describes the interaction of the cavity field with a two-level atom [57–59], and consists of the coherent annihilation of three photons accompanied by the excitation of the far-detuned atom [60,61] (four photons could be annihilated by employing a two-tone modulation [54]). Thus an amount of energy $\lesssim 2\hbar\omega_0$ could be extracted from the system due to resonant perturbation of some parameter, where $\omega_0$ is the cavity frequency [55]. However, in the more accessible regime of weak atom-field interaction (beneath the ultrastrong-coupling regime) the associated transition rate is quite small, so the

*adodonov@fis.unb.br

 

modulation frequency must be finely tuned and the dissipation strongly affects the behavior [54,55].

In this paper we uncover that the ADCE rate can be enhanced by more than one order of magnitude by employing artificial three-level atoms (qutrits) in the standard ladder configuration and weak-coupling regime [39]. We obtain a closed approximate description of the unitary dynamics when one or more atomic parameters undergo a low-amplitude multitone external perturbation, and assess the advantages and disadvantages of different regimes of parameters for the initial thermal state of the cavity field. We also discuss eventual complications that qutrits bring into the problem, such as adjustment of atomic energy levels with respect to the cavity frequency and two-tone driving with management of the modulation phases. Nevertheless it is argued that the substantial gain in the ADCE rate compensates for the additional technical issues.

This paper is organized as follows. In Sec. II we define our problem and derive the general mathematical formalism to obtain approximate expressions for the system dynamics in the dressed-states basis. In Sec. III we discuss three specific configurations of the qutrit for which the overall behavior is most easily inferred: the double-resonant, dispersive, and mixed regimes. In Sec. IV we identify the regimes of parameters and the transitions for which excitations can be annihilated from the cavity thermal state, assuming that the atom was initially in the lowest energy state. In Sec. V we evaluate analytically the transition rates associated with ADCE between different dressed states and compare our predictions to the exact numerical solution of the Schrödinger equation, demonstrating that the ADCE rate can undergo almost 50-fold increase compared to the qubit's case while the number of annihilated excitations is roughly the same. Our conclusions are summarized in Sec. VI.

## II. MATHEMATICAL FORMALISM

We consider a three-level artificial atom (qutrit) interacting with a single-cavity mode of constant frequency $\omega_0$, as described by the Hamiltonian (we set $\hbar = 1$)

$$\hat{H} = \omega_0 \hat{n} + \sum_{k=1}^{2} E_k \hat{\sigma}_{k,k} + \sum_{k=0}^{1} G_k (\hat{a} + \hat{a}^\dagger)(\hat{\sigma}_{k+1,k} + \hat{\sigma}_{k,k+1}). \tag{1}$$

$\hat{a}$ ($\hat{a}^\dagger$) is the cavity annihilation (creation) operator and $\hat{n} = \hat{a}^\dagger \hat{a}$ is the photon number operator. The atomic eigenenergies are $E_0 \equiv 0, E_1$, and $E_2$, with the corresponding states denoted as $|\mathbf{0}\rangle, |\mathbf{1}\rangle, |\mathbf{2}\rangle$; the atomic operators read $\hat{\sigma}_{k,j} \equiv |\mathbf{k}\rangle\langle\mathbf{j}|$. The parameters $G_k$ ($k = 0,1$) stand for the coupling strengths between the atomic states $\{|\mathbf{k}\rangle, |\mathbf{k}+\mathbf{1}\rangle\}$ mediated by the cavity field.

We assume that all the atomic parameters can be modulated externally as

$$E_k(t) \equiv E_{0,k} + \varepsilon_{E,k} f_{E,k}(t), \quad G_k(t) \equiv G_{0,k} + \varepsilon_{G,k} f_{G,k}(t),$$

where $\{\varepsilon_{E,k}, \varepsilon_{G,k}\}$ are the modulation depths and $\{E_{0,k}, G_{0,k}\}$ are the corresponding bare values. The dimensionless functions

$$f_l(t) = \sum_j w_l^{(j)} \sin\left(\eta^{(j)} t + \phi_l^{(j)}\right) \tag{2}$$

represent the externally prescribed modulation, where the collective index $l$ denotes $\{E; k = 1,2\}$ or $\{G; k = 0,1\}$. Constants $0 \leqslant w_l^{(j)} \leqslant 1$ and $\phi_l^{(j)}$ are the weight and the phase corresponding to the harmonic modulation of $l$ with frequency $\eta^{(j)}$, and the index $j$ runs over all the imposed frequencies (in this paper at most 2-tone modulations will be examined). We normalize the weights so that $\sum_j w_l^{(j)} = 1$ for any set $l$, so that $\varepsilon_l$ characterizes completely the modulation strength (in our examples we shall set $w_l^{(j)} = 1$ and $\phi_l^{(j)} = 0$ unless stated otherwise).

To obtain a closed analytical description we first rewrite the Hamiltonian as $\hat{H} = \hat{H}_0 + \hat{H}_c$, where

$$\hat{H}_0 = \omega_0 \hat{n} + \sum_{k=0}^{2} [E_{0,k} \hat{\sigma}_{k,k} + G_{0,k}(\hat{a}\hat{\sigma}_{k+1,k} + \hat{a}^\dagger \hat{\sigma}_{k,k+1})] \tag{3}$$

is the bare Hamiltonian in the absence of modulation and counter-rotating terms (to shorten the formulas we defined formally $G_{0,2} = \varepsilon_{G,2} = 0$). For the realistic *weak-coupling* regime ($G_{0,0}, G_{0,1} \ll \omega_0$) we expand the wave function corresponding to the total Hamiltonian $\hat{H}$ as

$$|\psi(t)\rangle = \sum_{n=0}^{\infty} \sum_{\mathcal{S}(n)} e^{-it\lambda_{n,\mathcal{S}}} A_{n,\mathcal{S}}(t) |\varphi_{n,\mathcal{S}}\rangle, \tag{4}$$

where $\lambda_{n,\mathcal{S}}$ and $|\varphi_{n,\mathcal{S}}\rangle$ are the $n$-excitation eigenvalues and eigenstates (*dressed states*) of the Hamiltonian $\hat{H}_0$ and the index $\mathcal{S}$ labels different states with a fixed number of excitations $n$, which is the quantum number associated with the operator $\hat{N} = \hat{n} + |\mathbf{1}\rangle\langle\mathbf{1}| + 2|\mathbf{2}\rangle\langle\mathbf{2}|$. As shown in Sec. III, the range of values of $\mathcal{S}$ depends on $n$, and we denote such degeneration with $g(n)$. Moreover, the number of excitations in the subspace coincides with the number of photons of the state having the atom in its ground ($|\mathbf{0}, n\rangle$).

Following the approach detailed in [31,61] we propose a change of variables that maps each group of $g(m)$ variables $A_{m,\mathcal{T}}$ into another set $b_{m,\mathcal{T}}$, so that $A_{m,\mathcal{T}} = \sum_{\mathcal{T}'} \alpha_{\mathcal{T}\mathcal{T}'} b_{m,\mathcal{T}'}$. In particular, we consider the following transformation:

$$\begin{aligned} A_{m,\mathcal{T}} = e^{i\Phi_{m,\mathcal{T}}(t)} \Bigg\{ & e^{-it\nu_{m,\mathcal{T}}} b_{m,\mathcal{T}}(t) \\ & - \frac{1}{2i} \sum_{\mathcal{S}(m) \neq \mathcal{T}} e^{-it\nu_{m,\mathcal{S}}} b_{m,\mathcal{S}}(t) \\ & \times {\sum_j}' \sum_{k=0}^{2} \sum_{L=E,G} \Upsilon_{m,\mathcal{T},\mathcal{S}}^{L,k,j} \\ & \times \sum_{r=\pm} e^{ri\phi_{L,k}^{(j)}} \frac{e^{it(\lambda_{m,\mathcal{T}} - \lambda_{m,\mathcal{S}} + r\eta^{(j)})} - 1}{\lambda_{m,\mathcal{T}} - \lambda_{m,\mathcal{S}} + r\eta^{(j)}} \Bigg\}, \end{aligned} \tag{5}$$

$$\begin{aligned} \Phi_{m,\mathcal{T}}(t) = & \sum_j \sum_{k=0}^{2} \sum_{L=E,G} \frac{\Upsilon_{m,\mathcal{T},\mathcal{T}}^{L,k,j}}{\eta^{(j)}} \\ & \times \left[ \cos\left(\eta^{(j)} t + \phi_{L,k}^{(j)}\right) - \cos \phi_{L,k}^{(j)} \right], \end{aligned} \tag{6}$$

where we divided the sum in two parts: $\sum_j'$ runs over "fast" frequencies $\eta^{(j')} \sim \lambda_{m+2,\mathcal{S}} - \lambda_{m,\mathcal{T}}$ and $\sum_j''$ runs over the "slow" ones $\eta^{(j'')} \sim |\lambda_{m,\mathcal{S}} - \lambda_{m,\mathcal{T}}|$. The small frequency shift $\nu_{m,\mathcal{T}}$ will be given in Eq. (13) and we introduced constant coefficients ($k = 0,1,2$)

$$\Upsilon^{E,k,j}_{m,\mathcal{T},\mathcal{S}} \equiv \varepsilon_{E,k} w^{(j)}_{E,k} \langle \varphi_{m,\mathcal{T}} | \hat{\sigma}_{k,k} | \varphi_{m,\mathcal{S}} \rangle, \tag{7}$$

$$\Upsilon^{G,k,j}_{m,\mathcal{T},\mathcal{S}} \equiv \varepsilon_{G,k} w^{(j)}_{G,k} \langle \varphi_{m,\mathcal{T}} | (\hat{a}\hat{\sigma}_{k+1,k} + \hat{a}^\dagger \hat{\sigma}_{k,k+1}) | \varphi_{m,\mathcal{S}} \rangle. \tag{8}$$

After substituting $A_{m,\mathcal{T}}$ into the Schrödinger equation and systematically eliminating the rapidly oscillating terms via the rotating wave approximation (RWA) [31], to the first order in $\varepsilon_{E,k}$ and $\varepsilon_{G,k}$ we obtain the approximate differential equation for the effective probability amplitude

$$\begin{aligned} \dot{b}_{m,\mathcal{T}} = & \sum_{\mathcal{S}(m)\neq\mathcal{T}} \varsigma_{m,\mathcal{T},\mathcal{S}} e^{it(\tilde{\lambda}_{m,\mathcal{T}} - \tilde{\lambda}_{m,\mathcal{S}})} b_{m,\mathcal{S}} \\ & + \sum_j'' \sum_{\mathcal{S}(m)\neq\mathcal{T}} \Xi^{(j)}_{m,\mathcal{T},\mathcal{S}} e^{it\varpi_{m,\mathcal{T},\mathcal{S}}(|\tilde{\lambda}_{m,\mathcal{T}} - \tilde{\lambda}_{m,\mathcal{S}}| - \eta^{(j)})} b_{m,\mathcal{S}} \\ & + \sum_j' \left[ \sum_{\mathcal{S}(m+2)} \Theta^{(j)}_{m+2,\mathcal{T},\mathcal{S}} e^{-it(\tilde{\lambda}_{m+2,\mathcal{S}} - \tilde{\lambda}_{m,\mathcal{T}} - \eta^{(j)})} b_{m+2,\mathcal{S}} \right. \\ & \left. - \sum_{\mathcal{S}(m-2)} \Theta^{(j)*}_{m,\mathcal{S},\mathcal{T}} e^{it(\tilde{\lambda}_{m,\mathcal{T}} - \tilde{\lambda}_{m-2,\mathcal{S}} - \eta^{(j)})} b_{m-2,\mathcal{S}} \right]. \end{aligned} \tag{9}$$

The time-independent transition rates between the dressed states are

$$\varsigma_{m,\mathcal{T},\mathcal{S}} = i \sum_{k,l=0}^{1} G_{0,k} G_{0,l} \left\{ \sum_{\mathcal{R}(m+2)} \frac{\Lambda_{k,m+2,\mathcal{T},\mathcal{R}} \Lambda_{l,m+2,\mathcal{S},\mathcal{R}}}{\lambda_{m+2,\mathcal{R}} - \lambda_{m,\mathcal{S}}} - \sum_{\mathcal{R}(m-2)} \frac{\Lambda_{k,m,\mathcal{R},\mathcal{T}} \Lambda_{l,m,\mathcal{R},\mathcal{S}}}{\lambda_{m,\mathcal{S}} - \lambda_{m-2,\mathcal{R}}} \right\},$$

$$\Xi^{(j)}_{m,\mathcal{T},\mathcal{S}} = \frac{\varpi_{m,\mathcal{T},\mathcal{S}}}{2} \sum_{k=0}^{2} \sum_{L=E,G} \Upsilon^{L,k,j}_{m,\mathcal{T},\mathcal{S}} e^{-i\varpi_{m,\mathcal{T},\mathcal{S}} \phi^{(j)}_{L,k}},$$

$$\begin{aligned} \Theta^{(j)}_{m+2,\mathcal{T},\mathcal{S}} = & \sum_{k=0}^{1} \frac{G_{0,k}}{2} \left\{ -\frac{\varepsilon^{(j)}_{G,k} \Lambda_{k,m+2,\mathcal{T},\mathcal{S}}}{G_{0,k}} \right. \\ & + \sum_{l=0}^{2} \sum_{L=E,G} \left[ \sum_{\mathcal{R}(m+2)} \frac{\Lambda_{k,m+2,\mathcal{T},\mathcal{R}} \Upsilon^{L,l,j}_{m+2,\mathcal{R},\mathcal{S}} e^{i\phi^{(j)}_{L,l}}}{\lambda_{m+2,\mathcal{R}} - \lambda_{m+2,\mathcal{S}} + \eta^{(j)}} \right. \\ & \left. \left. - \sum_{\mathcal{R}(m)} \frac{\Lambda_{k,m+2,\mathcal{R},\mathcal{S}} \Upsilon^{L,l,j}_{m,\mathcal{T},\mathcal{R}} e^{i\phi^{(j)}_{L,l}}}{\lambda_{m,\mathcal{T}} - \lambda_{m,\mathcal{R}} + \eta^{(j)}} \right] \right\}, \end{aligned} \tag{10}$$

$$\Lambda_{k,m+2,\mathcal{T},\mathcal{S}} = \langle \varphi_{m,\mathcal{T}} | \hat{a}\hat{\sigma}_{k,k+1} | \varphi_{m+2,\mathcal{S}} \rangle. \tag{11}$$

Here $\varpi_{m,\mathcal{T},\mathcal{S}} \equiv \mathrm{sgn}(\tilde{\lambda}_{m,\mathcal{T}} - \tilde{\lambda}_{m,\mathcal{S}})$ and we introduced the complex modulation depth $\varepsilon^{(j)}_l \equiv \varepsilon_l w^{(j)}_l \exp(i\phi^{(j)}_l)$. Moreover, we defined the corrected eigenfrequencies

$$\tilde{\lambda}_{m,\mathcal{T}} \equiv \lambda_{m,\mathcal{T}} + \nu_{m,\mathcal{T}} + \Delta\nu, \tag{12}$$

where the correction due to counter-rotating terms reads

$$\nu_{m,\mathcal{T}} = \left[ \sum_{\mathcal{S}(m-2)} \frac{\left(\sum_{k=0}^{1} G_{0,k} \Lambda_{k,m,\mathcal{S},\mathcal{T}}\right)^2}{\lambda_{m,\mathcal{T}} - \lambda_{m-2,\mathcal{S}}} - \sum_{\mathcal{S}(m+2)} \frac{\left(\sum_{k=0}^{1} G_{0,k} \Lambda_{k,m+2,\mathcal{T},\mathcal{S}}\right)^2}{\lambda_{m+2,\mathcal{S}} - \lambda_{m,\mathcal{T}}} \right] \tag{13}$$

and $\Delta\nu$ denotes the neglected contributions smaller than $\nu_{m,\mathcal{T}}$ and the terms of the order $\sim(\Upsilon^{L,k,j}_{m,\mathcal{T},\mathcal{S}})^2/\omega_0, (\varepsilon_{G,k}\Lambda_{k,m,\mathcal{S},\mathcal{T}})^2/\omega_0$.

Throughout the derivation of the formula (9) we have assumed the constraints

$$|\lambda_{m,\mathcal{T}} - \lambda_{m,\mathcal{S}}|, \left|\Upsilon^{L,k,j}_{m,\mathcal{T},\mathcal{S}}\right|, \left|\frac{G_{0,k}\Lambda_{l,m,\mathcal{S},\mathcal{T}}}{\lambda_{m+2,\mathcal{T}} - \lambda_{m,\mathcal{S}}}\right| G_{0,l} \ll \omega_0, \tag{14}$$

$$G_{0,k} |\Lambda_{k,m+2,\mathcal{S},\mathcal{T}}| \lesssim \omega_0.$$

Under these approximations we have $|A_{m,\mathcal{T}}| \approx |b_{m,\mathcal{T}}|$, so from Eq. (9) one can easily infer the evolution of populations of the dressed states. Besides, the generalization of our method for $N$-level atoms and second-order effects is straightforward [61].

It is worth noting that the occurrence of ADCE is essentially governed by the transition rates $\Theta^{(j)}_{m,\mathcal{T},\mathcal{S}}$ that couple states belonging to subspaces with different numbers of excitations. Of course the whole dynamics is determined also by the transitions occurring inside each subspace, but the annihilation of (two) excitations is possible only in the presence of non-negligible $\Theta$ terms.

## III. ANALYTICAL REGIMES

We shall confine ourselves to three different regimes of parameters for which the dressed states have simple analytical expressions. With the aid of these formulas we shall be able to evaluate analytically the coefficients $\Theta^{(j)}_{m,\mathcal{S},\mathcal{T}}$ in Sec. IV.

The ground state of $\hat{H}_0$ is $|\varphi_0\rangle = |\mathbf{0},0\rangle$ and the corresponding eigenenergy is $\lambda_0 = 0$. In this paper we denote $|\mathbf{k},n\rangle \equiv |\mathbf{k}\rangle_{\mathrm{atom}} \otimes |n\rangle_{\mathrm{field}}$, where $\mathbf{k}$ stands for the atomic level and $n$ stands for the Fock state. Moreover, we define the bare atomic transition frequencies as

$$\Omega_{01} = E_{0,1} - E_{0,0} \equiv \omega_0 - \Delta_1,$$
$$\Omega_{12} = E_{0,2} - E_{0,1} \equiv \omega_0 - \Delta_2,$$

where $\Delta_1$ and $\Delta_2$ are the bare detunings.

### A. Two-level atom

We include this case ($G_{0,1} = 0$) to compare the advantages and disadvantages of using qutrits instead of qubits. The exact expressions for $m \geqslant 1$ read

$$\lambda_{m,\pm D} = \omega_0 m - \frac{\Delta_1}{2} \pm D\frac{\beta_m}{2}, \tag{15}$$

$$|\varphi_{m,\pm D}\rangle = \frac{1}{\sqrt{\beta_m}} [\sqrt{\beta_{m,\pm}} |\mathbf{0},m\rangle \pm D\sqrt{\beta_{m,\mp}} |\mathbf{1},m-1\rangle], \tag{16}$$

where $\beta_m = \sqrt{\Delta_1^2 + 4G_{0,0}^2 m}$, $\beta_{m,\pm} = (\beta_m \pm |\Delta_1|)/2$ and we introduced the *detuning symbol* $D = +1$ for $\Delta_1 \geqslant 0$ and $D = -1$ for $\Delta_1 < 0$.

For the qutrits we can use Eqs. (15) and (16) for the subspace containing a single excitation, $m = 1$; the dressed states with $m \geqslant 2$ excitations are presented below.

### B. Double-resonant regime

When both $G_{0,0}$ and $G_{0,1}$ are nonzero, first we consider the special case when $\Delta_2 = -\Delta_1$, so that we have the "double resonance" $\Omega_{02} = E_{0,2} - E_{0,0} = 2\omega_0$. The exact formulas read (for $m \geqslant 2$)

$$\lambda_{m,0} = m\omega_0, \lambda_{m,\pm D} = m\omega_0 \pm D\varrho_{m,\mp}, \tag{17}$$

$$|\varphi_{m,0}\rangle = \mathcal{N}_{m,0}^{-1}[-G_{0,1}\sqrt{m-1}|\mathbf{0},m\rangle + \sqrt{m}G_{0,0}|\mathbf{2},m-2\rangle],$$

$$|\varphi_{m,\pm D}\rangle = \mathcal{N}_{m,\mp}^{-1}[\sqrt{m}G_{0,0}|\mathbf{0},m\rangle \pm D\varrho_{m,\mp}|\mathbf{1},m-1\rangle + \sqrt{m-1}G_{0,1}|\mathbf{2},m-2\rangle],$$

where we defined

$$\varrho_m = \sqrt{\Delta_1^2/4 + mG_{0,0}^2 + (m-1)G_{0,1}^2},$$

$$\varrho_{m,\pm} = \varrho_m \pm |\Delta_1|/2, \varrho_{m,0} = \sqrt{mG_{0,0}^2 + (m-1)G_{0,1}^2},$$

$$\mathcal{N}_{m,0} = \varrho_{m,0}, \mathcal{N}_{m,\pm} = \sqrt{2\varrho_m\varrho_{m,\pm}}.$$

For example, if $G_{0,1} \sim G_{0,0}$ and $|\Delta_1| \gg G_{0,0}\sqrt{n}$ for all relevant values of $n$ we have approximately $|\varphi_{m,-D}\rangle \sim |\mathbf{1},m-1\rangle$, $|\varphi_{m,0}\rangle \sim (|\mathbf{0},m\rangle - |\mathbf{2},m-2\rangle)/\sqrt{2}$, and $|\varphi_{m,D}\rangle \sim (|\mathbf{0},m\rangle + |\mathbf{2},m-2\rangle)/\sqrt{2}$. On the other hand, for $|\Delta_1| \ll G_{0,0}, G_{0,1}$ (near the atom-field resonance) we get $|\varphi_{m,\pm D}\rangle \sim (|\mathbf{0},m\rangle \pm \sqrt{2}|\mathbf{1},m-1\rangle + |\mathbf{2},m-2\rangle)/2$.

### C. Dispersive regime

Now we assume that both the atomic transition frequencies are far-detuned from the cavity frequency

$$|\Delta_1|, |\Delta_2|, |\Delta_1 + \Delta_2| \gg G_{0,0}\sqrt{m}, G_{0,1}\sqrt{m-1}. \tag{18}$$

From the perturbation theory we obtain to the fourth order in $G_{0,0}/\Delta_1$ and $G_{0,1}/\Delta_2$

$$\lambda_{m,0} = m\omega_0 + \delta_1 m\left[1 + \frac{G_{0,1}^2(m-1)}{\Delta_1(\Delta_1+\Delta_2)} - \frac{G_{0,0}^2 m}{\Delta_1^2}\right],$$

$$|\varphi_{m,0}\rangle = \mathcal{N}_{m,0}^{-1}\left[|\mathbf{0},m\rangle + \frac{\rho_{m,0}G_{0,0}\sqrt{m}}{\Delta_1}|\mathbf{1},m-1\rangle + \frac{r_{m,0}G_{0,0}G_{0,1}\sqrt{m(m-1)}}{\Delta_1(\Delta_1+\Delta_2)}|\mathbf{2},m-2\rangle\right],$$

$$\lambda_{m,1} = m\omega_0 - \Delta_1 - [\delta_1 m - \delta_2(m-1)] \times\left[1 - \frac{G_{0,0}^2 m}{\Delta_1^2} - \frac{G_{0,1}^2(m-1)}{\Delta_2^2}\right],$$

$$|\varphi_{m,1}\rangle = \mathcal{N}_{m,1}^{-1}\left[|\mathbf{1},m-1\rangle - \frac{\rho_{m,1}G_{0,0}\sqrt{m}}{\Delta_1}|\mathbf{0},n\rangle + \frac{r_{m,1}G_{0,1}\sqrt{m-1}}{\Delta_2}|\mathbf{2},m-2\rangle\right],$$

$$\lambda_{m,2} = m\omega_0 - \Delta_1 - \Delta_2 - \delta_2(m-1) \times\left[1 + \frac{G_{0,0}^2 m}{\Delta_2(\Delta_1+\Delta_2)} - \frac{G_{0,1}^2(m-1)}{\Delta_2^2}\right],$$

$$|\varphi_{m,2}\rangle = \mathcal{N}_{m,2}^{-1}\left[|\mathbf{2},m-2\rangle - \frac{\rho_{m,2}G_{0,1}\sqrt{m-1}}{\Delta_2}|\mathbf{1},m-1\rangle + \frac{r_{m,2}G_{0,0}G_{0,1}\sqrt{m(m-1)}}{\Delta_2(\Delta_1+\Delta_2)}|\mathbf{0},m\rangle\right],$$

where we defined the dispersive shifts $\delta_1 \equiv G_{0,0}^2/\Delta_1$ and $\delta_2 \equiv G_{0,1}^2/\Delta_2$. We adopted an intuitive notation in which the second index in $|\varphi_{m,\mathcal{S}}\rangle$ represents the most probable atomic state in a given dressed state (for example, in the expansion of $|\varphi_{m,0}\rangle$ the bare state $|\mathbf{0},m\rangle$ appears with the highest weight). The parameters $\rho_{m,\mathcal{S}}$, $r_{m,\mathcal{S}}$, and $\mathcal{N}_{m,\mathcal{S}}$ are equal to 1 to the first order in $G_{0,0}/\Delta_1$, $G_{0,1}/\Delta_2$ and their expressions are reported in Sec. I of the Supplemental Material [62].

### D. Mixed regime

In the mixed regime we assume $\Delta_2 = 0$ and

$$|\Delta_1| \gg G_{0,0}\sqrt{n},\ G_{0,1}\sqrt{n-1}; \tag{19}$$

i.e., the atomic transition $|\mathbf{1}\rangle \to |\mathbf{2}\rangle$ is resonant with the cavity mode, while the transition $|\mathbf{0}\rangle \to |\mathbf{1}\rangle$ is far-detuned. To the second order in $G_{0,0}/\Delta_1$ we obtain

$$\lambda_{m,0} = m\omega_0 + \frac{\Delta_1 G_{0,0}^2 m}{\Delta_1^2 - G_{0,1}^2(m-1)},$$

$$|\varphi_{m,0}\rangle = \mathcal{N}_{m,0}^{-1}\{G_{0,1}\sqrt{m-1}\rho_{m,0}|\mathbf{2},m-2\rangle + \rho_{m,0}\Delta_1|\mathbf{1},m-1\rangle + |\mathbf{0},m\rangle\},$$

$$\lambda_{m,\pm D} = m\omega_0 - D\left(|\Delta_1| \mp G_{0,1}\sqrt{m-1} + \frac{1}{2}\frac{G_{0,0}^2 m}{|\Delta_1| \mp G_{0,1}\sqrt{m-1}}\right),$$

$$|\varphi_{m,\pm D}\rangle = \mathcal{N}_{m,\pm}^{-1}\{(1-r_{m,\pm})|\mathbf{2},m-2\rangle \pm D(1+r_{m,\pm})|\mathbf{1},m-1\rangle + \rho_{m,\pm}|\mathbf{0},m\rangle\},$$

where we defined

$$\rho_{m,\pm} = \frac{G_{0,0}\sqrt{m}}{G_{0,1}\sqrt{m-1} \mp |\Delta_1|},\ \rho_{m,0} = \frac{G_{0,0}\sqrt{m}}{\Delta_1^2 - G_{0,1}^2(m-1)},$$

$$r_{m,\pm} = \frac{1}{4}\frac{G_{0,0}^2 m}{G_{0,1}\sqrt{m-1}(G_{0,1}\sqrt{m-1} \mp |\Delta_1|)},$$

$$\mathcal{N}_{m,0} = \sqrt{1 + \rho_{n,0}^2\left[\Delta_1^2 + (m-1)G_{0,1}^2\right]},$$

$$\mathcal{N}_{m,\pm} = \sqrt{2 + 2r_{m,\pm}^2 + \rho_{m,\pm}^2}\,.$$

## IV. ADCE

Our goal is to study the coherent annihilation of system excitations from the initial separable state $\hat{\rho}_0 = |\mathbf{0}\rangle\langle\mathbf{0}| \otimes \hat{\rho}_{th}$, where $\hat{\rho}_{th} = \sum_{m=0}^{\infty} \rho_m |m\rangle\langle m|$ is the cavity *thermal state* with $\rho_m = \bar{n}^m/(\bar{n}+1)^{m+1}$. Here $\bar{n} = (e^{\omega\beta} - 1)^{-1}$ is the average initial photon number, $\beta^{-1} = k_B T$, $T$ is the absolute temperature, and $k_B$ is the Boltzmann constant. From Eq. (10) it is clear that such process can be implemented via transition of the form $|\varphi_{m,\mathcal{T}}\rangle \to |\varphi_{m-2,\mathcal{S}}\rangle$ when the modulation frequency is $\eta^{(\mathrm{res})} = \tilde{\lambda}_{m,\mathcal{T}} - \tilde{\lambda}_{m-2,\mathcal{S}}$. So first we must determine the dressed states for which the initial population of the state $|\varphi_{m,\mathcal{T}}\rangle$, denoted as $P_{m,\mathcal{T}}$, is larger than $P_{m-2,\mathcal{S}}$. We assume a small integer $m$ (for the sake of illustration we choose $m = 4$, although the overall behavior is similar for other values of $m$) and set the realistic parameters $G_{0,0} = 6 \times 10^{-2}\omega_0$ and $\bar{n} = 1.5$. We verified numerically that when $G_{0,1}$ is of the same order of $G_{0,0}$ the exact value of $G_{0,1}$ does not affect qualitatively the results, so in this paper we set $G_{0,1} = 1.2G_{0,0}$. See Sec. II of the Supplemental Material [62] for an illustration of the quantitative differences in the results when $G_{0,1} = G_{0,0}$ or $G_{0,1} = 0.8G_{0,0}$.

In Fig. 1 we plot the initial population difference $P(m,\mathcal{T},\mathcal{S}) \equiv P_{m,\mathcal{T}} - P_{m-2,\mathcal{S}}$ as a function of $|\Delta_1|$ for $m = 4$. Only positive values of $P(4,\mathcal{T},\mathcal{S})$ are plotted and the values $(\mathcal{T},\mathcal{S})$ are indicated next to the curves, where the index stands for 2-level (2L), double-resonant (r), dispersive (d), and mixed (m) regimes. In the dispersive and mixed regimes we assume $|\Delta_1|/G_{0,0} \geqslant 4$ in order to satisfy the approximations (18) and (19). Besides, throughout this paper we set $\Delta_2 = 6G_{0,0}\mathrm{sgn}(\Delta_1)$ in the dispersive regime so that $|\Delta_1 + \Delta_2|$ never approaches zero, as required by the inequality (18). One can see that large detuning $|\Delta_1|$ favors the implementation of ADCE; the transitions $(1,2)_d$ and $(D,-D)_m$ are not particularly useful since the population differences are always small and are inversely proportional to the detuning. As already known, for a qubit the ADCE relies on the transition $(D,-D)_{2L}$. From Fig. 1 we discover that for a qutrit we have the following candidates for the realization of ADCE: $(D,-D)_r$ and $(0,-D)_r$ in the double-resonant regime, $(0,1)_d$ and $(0,2)_d$ in the dispersive regime, and $(0,D)_m$ and $(0,-D)_m$ in the mixed regime.

Now we are in position to evaluate the ADCE rate in different regimes according to Eq. (10). For the transition $|\varphi_{m,\mathcal{T}}\rangle \to |\varphi_{m-2,\mathcal{S}}\rangle$ [denoted as $(T,S)$] we evaluate analytically $\Theta_{m,\mathcal{S},\mathcal{T}}$ under the resonant modulation frequency $\eta^{(\mathrm{res})} = \tilde{\lambda}_{m,\mathcal{T}} - \tilde{\lambda}_{m-2,\mathcal{S}}$. In Fig. 2(a) we plot the dimensionless transition rate $|\Theta_{m,\mathcal{S},\mathcal{T}}|/\omega_0$ for $m = 4$ assuming the harmonic modulation of $E_1$ with perturbative amplitude $\varepsilon_{E,1} = 5 \times 10^{-2}\Omega_{01}$. We disregard the region near $\Delta_1 = 0$ since $P(m,\mathcal{T},\mathcal{S}) < 0$ in this case, so ADCE does not occur. We observe that for the qutrit in the dispersive or mixed

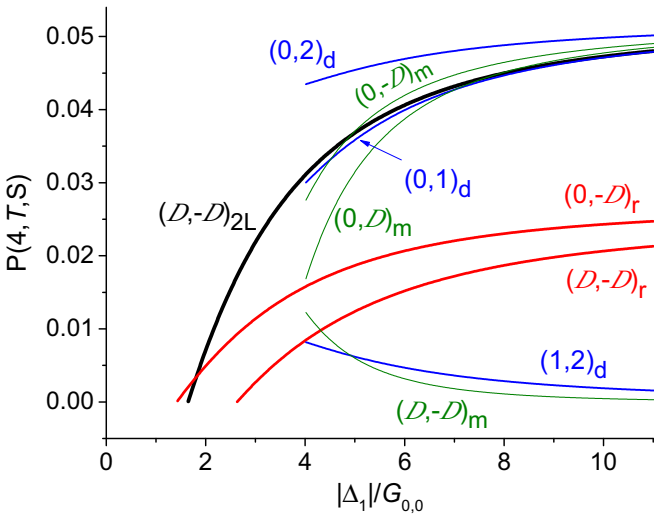


FIG. 1. Difference of initial populations $P(m,\mathcal{T},\mathcal{S}) \equiv P_{m,\mathcal{T}} - P_{m-2,\mathcal{S}}$ for $m = 4$ and different regimes as function of the absolute value of the detuning $\Delta_1$. Regimes: 2-level atom (2L), double-resonant regime (r), dispersive regime (d), and mixed regime (m). Only the states for which $P(m,\mathcal{T},\mathcal{S}) > 0$ are plotted and the values $(\mathcal{T},\mathcal{S})$ are indicated alongside the curves. (Here $G_{0,1} = 1.2G_{0,0}$.)

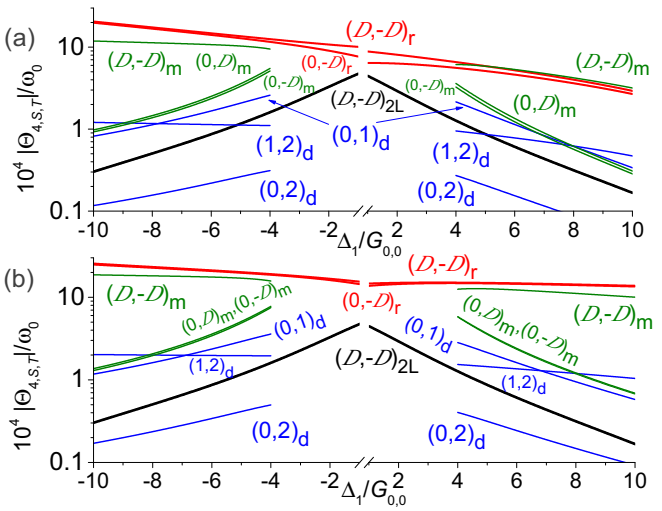


FIG. 2. (a) Transition rate for ADCE (involving the transition $|\varphi_{4,\mathcal{T}}\rangle \to |\varphi_{2,\mathcal{S}}\rangle$) as a function of $\Delta_1/G_{0,0}$ for $m = 4$ and modulation of $E_1$. The values of indexes $(\mathcal{T},\mathcal{S})$ are indicated alongside the curves in different regimes. (b) Same as (a) but for the simultaneous modulation of $E_1$ and $E_2$ with the same frequency. In the dispersive regime (d) we set $\Delta_2 = 6G_{0,0}\mathrm{sgn}(\Delta_1)$. In the mixed regime (m) the lines $(0,D)$ and $(0,-D)$ are very close, so for the sake of compactness they are not discerned separately. We do not show the transition rate near $|\Delta_1| = 0$, since all the population differences $P(m,\mathcal{T},\mathcal{S})$ are negative in this case. Notice the increment by at least one order of magnitude of the transition rate in the double-resonant regime (r) [compared to the qubit's case (2L)] for $|\Delta_1| \gg G_{0,0}$.

regimes the transition rates can be slightly higher than for the qubit; the rate for the transition $(D,-D)_m$ is substantially higher than for the qubit; however this transition is not useful for ADCE due to small population difference $P(m,D,-D)$. We also note that in the dispersive regime one can induce the transition $|\varphi_{m,0}\rangle \to |\varphi_{m-2,2}\rangle$ for modulation frequency $\eta^{(\mathrm{res})} \approx 4\omega_0 - \Omega_{02}$, which corresponds approximately to the *four-photon transition* $|\mathbf{0},m\rangle \to |\mathbf{2},m-4\rangle$. However the associated transition rate is even smaller than the ADCE rate for a qubit, hindering practical applications of such process.

In the dispersive regime the transition rate and the population difference for the process $|\varphi_{m,0}\rangle \to |\varphi_{m-2,1}\rangle$ [denoted as $(0,1)_d$ in the figures] is roughly the same as the process $|\varphi_{m,D}\rangle \to |\varphi_{m-2,-D}\rangle$ for a qubit [denoted as $(D,-D)_{2L}$]. Therefore, the behavior of multilevel atoms with respect to ADCE is similar to the one for a qubit, provided all the transitions are far-detuned from the cavity frequency. Moreover, for the mixed regime and large detuning $|\Delta_1|$ the population differences $P(m,0,D)$ and $P(m,0,-D)$ are roughly the same as for the qubit, while the transition rates are several times larger, so the implementation of ADCE would be facilitated.

The main finding of the paper is the observation that in the double-resonant regime the ADCE rate is at least one order of magnitude larger than for the qubit, and the difference increases for larger $|\Delta_1|$, as can be seen from Fig. 2(a). Besides, in this regime the population differences $P(m,D,-D)$ and $P(m,0,-D)$ also increase proportionally to $|\Delta_1|$, achieving sufficiently large values for $|\Delta_1| \sim 8G_{0,0}$ (see Fig. 1). Thus, it seems that one could speed up ADCE by at least one order of magnitude using three-level atoms in the double-resonant configuration instead of qubits, provided the detuning $|\Delta_1|$ is large enough.

In real circuit QED setups it might be tricky to modulate only one parameter at a time, while keeping the other parameters constant. So in Fig. 2(b) we consider the simultaneous modulation of $E_1$ and $E_2$ (with the same modulation frequency $\eta^{(\mathrm{res})} = \tilde{\lambda}_{m,\mathcal{T}} - \tilde{\lambda}_{m-2,\mathcal{S}}$) assuming parameters $\varepsilon_{E,1} = 5\times 10^{-2}\Omega_{01}$, $\varepsilon_{E,2} = 5\times 10^{-2}\Omega_{12}$, $\phi_{E,1} = 0$, and $\phi_{E,2} = \pi$. Conveniently the ADCE transition rates increase even more when compared to an isolated modulation of either $E_1$ or $E_2$.

To give a rough estimation of the gain in the ADCE transition rate we evaluated analytically the $\Theta$ coefficients for the simultaneous modulation of $E_1$ and $E_2$, assuming similar coupling strengths ($G_{0,0} \sim G_{0,1}$) and large detunings ($|\Delta_1| \gg G_{0,0}\sqrt{m}$). For the qubit we recover the formula obtained in [34]

$$\left|\Theta^{(j)}_{m,-D,D}\right| \simeq \frac{G_{0,0}}{2}\left(\frac{G_{0,0}}{\Delta_1}\right)^2 \sqrt{m(m-1)(m-2)} \times \frac{\omega_0+\Delta_1}{\omega_0}\frac{\varepsilon_{E,1}w^{(j)}_{E,1}}{2\omega_0+\Delta_1},$$

while for the qutrits in the *double-resonant* regime we find

$$\left|\Theta^{(j)}_{m,-D,0}\right| \simeq \frac{G_{0,0}\sqrt{m}}{2}R^{(j)}_m,$$

$$\left|\Theta^{(j)}_{m,-D,D}\right| \simeq \frac{G_{0,1}\sqrt{m-1}}{2}R^{(j)}_m,$$

$$R^{(j)}_m \equiv \frac{G_{0,1}\sqrt{m-2}}{\sqrt{mG^2_{0,0}+(m-1)G^2_{0,1}}} \times \frac{\left|\varepsilon_{E,1}w^{(j)}_{E,1} - \varepsilon_{E,2}w^{(j)}_{E,2}e^{i(\phi^{(j)}_{E,2}-\phi^{(j)}_{E,1})}\right|}{2\omega_0+\Delta_1}.$$

Hence under the lone modulation of $E_1$ the utilization of qutrits instead of qubits increases the ADCE rate by a factor of the order of magnitude of

$$\mathcal{G} = \frac{\sqrt{2}}{2m-1}\left(\frac{\Delta_1}{G_{0,0}}\right)^2 \frac{\omega_0}{\omega_0+\Delta_1}. \tag{20}$$

Moreover, for the simultaneous modulation of $E_1$ and $E_2$, with $\varepsilon_{E,1}w^{(j)}_{E,1} \sim \varepsilon_{E,2}w^{(j)}_{E,2}$, there is an additional rise by a factor of 2 provided that $\phi^{(j)}_{E,2} - \phi^{(j)}_{E,1} \approx \pi$.

In Sec. III of the Supplemental Material [62] we illustrate in detail the transition rates and the population differences for different values of $G_{0,1}$ and isolated modulations of $E_2$, $G_0$, and $G_1$. It is found that the modulation of $G_0$ does not speed up significantly the transition rate in comparison to a qubit, whereas the modulation of $E_2$ or $G_1$ does increase the transition rate in the double-resonant regime by at least one order of magnitude. We also verified that under the simultaneous modulation of all the parameters ($E_1$, $E_2$, $G_0$, and $G_1$) the total transition rate is still substantially higher than for a qubit, provided the phases are properly adjusted. Hence, the simultaneous modulation of several parameters is not an issue from the experimental point of view, provided one can manage the phases $\phi^{(j)}_l$ corresponding to different modulation components.

## V. NUMERICAL VERIFICATION

Now we proceed to the numerical verification of the phenomenon predicted in the previous section, namely, the enhancement of the ADCE rate in the double-resonant regime. We solved numerically the Schrödinger equation for the Hamiltonian (1) using the initial local thermal state $\hat{\rho}_0 = |\mathbf{0}\rangle\langle\mathbf{0}| \otimes \hat{\rho}_{th}$ and parameters $m = 4$, $G_{0,0} = 6\times 10^{-2}\omega_0$, $G_{0,1} = 1.2G_{0,0}$, $\bar{n} = 1.5$, and $\Delta_1 = -\Delta_2 = -8G_{0,0}$. (Recall that $m$ denotes the subset of dressed states $|\varphi_{m,\mathcal{T}}\rangle$ with $m$ excitations from which the excitations will be annihilated. Since the state $\hat{\rho}_{th}$ has a nonvanishing overlap with the Fock state $|4\rangle$, relevant transitions will be involved in the dynamics.) One downside of using the double-resonant regime for qutrits is clear from Fig. 1: both the populations differences $(0,-D)_r$ and $(D,-D)_r$, involved in the ADCE, are roughly twice smaller than the population difference $(D,-D)_{2L}$ for the qubit. Hence, considering the connection between ADCE and quantum thermodynamic processes recently analyzed in Ref. [55], we can say that the work extraction would be half smaller if one used qutrits instead of qubits. This nuisance can be readily surpassed by employing 2-tone modulation with frequencies $\eta^{(1)} = \tilde{\lambda}_{m,0} - \tilde{\lambda}_{m-2,-D}$ and $\eta^{(2)} = \tilde{\lambda}_{m,D} - \tilde{\lambda}_{m-2,-D}$ that drives simultaneously the transitions $|\varphi_{m,0}\rangle \to |\varphi_{m-2,-D}\rangle$ and $|\varphi_{m,D}\rangle \to |\varphi_{m-2,-D}\rangle$.

In Fig. 3(a) we illustrate the dynamics of the average photon number $n_{ph} = \langle\hat{n}\rangle$, the average number of atomic excitations $n_{at} = \langle\sum_{k=1}^{2} k\hat{\sigma}_{k,k}\rangle$, and the total average num-

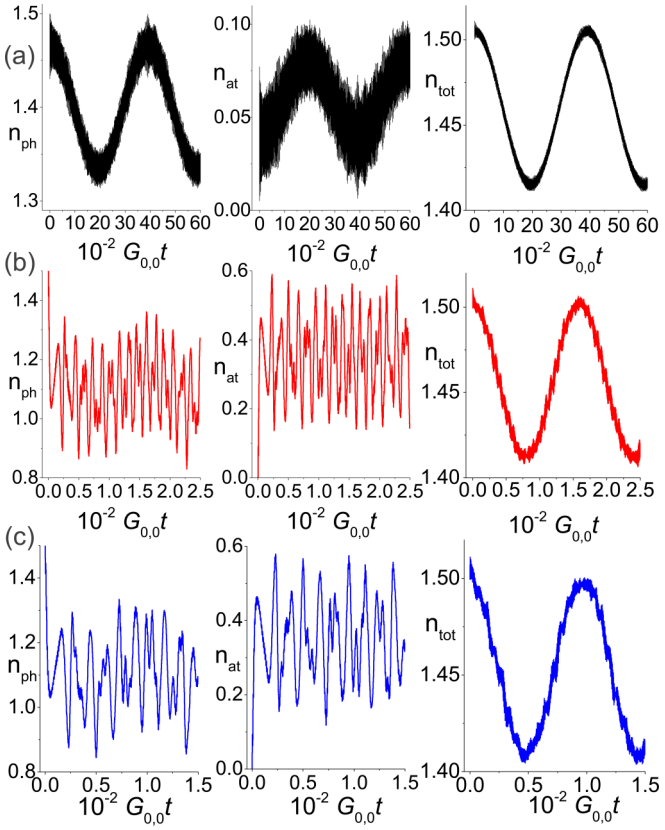


FIG. 3. Exact numerical dynamics of ADCE obtained for the Hamiltonian (1) and the initial local thermal state $\hat{\rho}_0$ in the double-resonant regime. (a) 2-level atom and harmonic modulation of $E_1$. (b) 3-level atom and 2-tone modulation of $E_1$. (c) 3-level atom and 2-tone double modulation of $E_1$ and $E_2$. Notice that in all cases the number of annihilated excitations $n_{\rm tot}$ is roughly the same, while the duration of the process in (c) is roughly 40 times smaller than in (a).

ber of excitations $n_{\rm tot} = n_{ph} + n_{at}$ for a qubit (setting momentarily $G_1 = 0$) with modulation depth $\varepsilon_{E,1} = 5 \times 10^{-2}\Omega_{01}$. We observe the sinusoidal oscillation of $n_{ph}, n_{at}$, and $n_{\rm tot}$ with typical period $\tau \approx 4 \times 10^3 G_{0,0}^{-1}$. The coherent annihilation of excitations does take place, but since the initial population of the state $|\varphi_{4,D}\rangle$ was $P_{4,D} \approx 5 \times 10^{-2}$, the average number of annihilated excitations is $\sim 2P_{m,D} \approx 0.1$, in agreement with the numerical data.

In Fig. 3(b) we consider the qutrit under 2-tone modulation of $E_1$ with the previous amplitude $\varepsilon_{E,1} = 5 \times 10^{-2}\Omega_{01}$, weights $w_{E,1}^{(1)} = 10/17, w_{E,1}^{(2)} = 7/17$, and phases $\phi_{E,1}^{(1)} = 0, \phi_{E,1}^{(2)} = \pi$ (the weights were adjusted to equalize the two transition rates). We see that the total number of excitations exhibits the same qualitative behavior as for the qubit, but the transition rate undergoes almost 30-fold increase. Such gain agrees with the theoretical estimate, Eq. (20), which gives $\mathcal{G} \approx 25$ for the present parameters. The behavior of $n_{ph}$ and $n_{at}$ differs drastically from the one observed for the 2-level atom partly due to the oscillations between the bare states $|\mathbf{0},k\rangle \leftrightarrow |\mathbf{2},k-2\rangle$ for $k \geqslant 2$, and partly due to the oscillations between the dressed states $|\varphi_{k,D}\rangle \leftrightarrow |\varphi_{k,0}\rangle$, as will be discussed shortly. In Fig. 3(c) we consider the simultaneous two-tone modulation of $E_1$ and $E_2$ with parameters $\varepsilon_{E,1} = 5 \times 10^{-2}\Omega_{01}, \varepsilon_{E,2} = 9 \times 10^{-2}\Omega_{12}, w_{E,1}^{(1)} = w_{E,2}^{(1)} = 10/17, w_{E,1}^{(2)} = w_{E,2}^{(2)} = 7/17$ and phases $\phi_{E,1}^{(1)} = \phi_{E,2}^{(2)} = 0, \phi_{E,1}^{(2)} = \phi_{E,2}^{(1)} = \pi$. We see that the ADCE rate suffers an additional 50% rise compared to the sole modulation of $E_1$, while the average number of total annihilated excitations is roughly the same as in the previous cases.

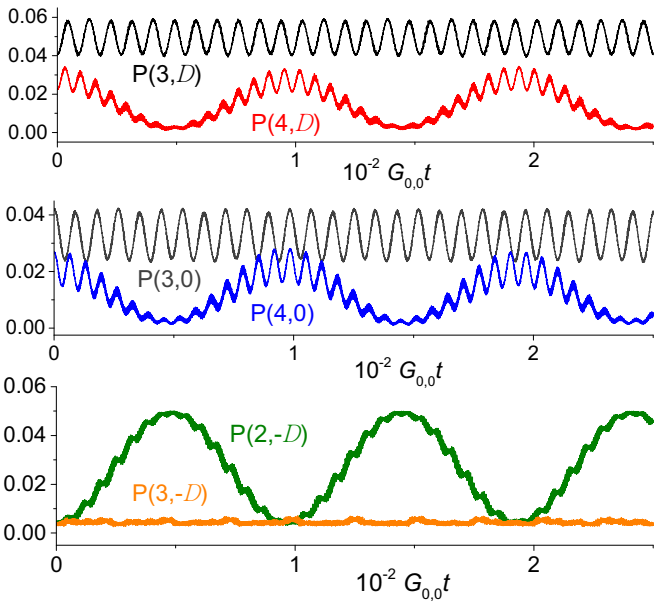


FIG. 4. Dynamics of populations of relevant dressed states for the 2-tone double modulation of $E_1$ and $E_2$ analyzed in Fig. 3(c). There is a coherent transfer of populations from the states $|\varphi_{4,D}\rangle$ and $|\varphi_{4,0}\rangle$ to the state $|\varphi_{2,-D}\rangle$. Moreover, one observes periodic oscillations between the dressed states $|\varphi_{k,D}\rangle \leftrightarrow |\varphi_{k,0}\rangle$ for $k \geqslant 2$ due to the counter-rotating terms in the Hamiltonian (1).

Finally, in Fig. 4 we plot the probabilities of finding the system in the dressed states $P(m,\mathcal{S}) = \mathrm{Tr}[\hat{\rho}(t)|\varphi_{m,\mathcal{S}}\rangle\langle\varphi_{m,\mathcal{S}}|]$ as a function of time for the 2-tone double modulation discussed in Fig. 3(c). As predicted by Eq. (9) there is a simultaneous periodic transfer of populations from the states $|\varphi_{4,D}\rangle$ and $|\varphi_{4,0}\rangle$ to the state $|\varphi_{2,-D}\rangle$, which corresponds to the coherent annihilation of two-system excitations. Other states $|\varphi_{k\neq 2,-D}\rangle$ are not affected by the modulation, as illustrated for the state $|\varphi_{3,-D}\rangle$ which undergoes just minor fluctuations due to off-resonant couplings neglected under RWA. Moreover, one also observes periodic oscillations between the dressed states $|\varphi_{k,D}\rangle \leftrightarrow |\varphi_{k,0}\rangle$ for $k \geqslant 2$. This occurs because for large $|\Delta_1|$ we have $\tilde{\lambda}_{k,0} \approx \tilde{\lambda}_{k,D}$, as seen from Eq. (17); hence the first term on the right-hand side of Eq. (9) becomes nearly resonant and couples these states with the strength $\sim|\varsigma_{k,D,0}|$ [this behavior is due solely to the counter-rotating terms in Eq. (1) and is independent of modulation].

## VI. CONCLUSIONS

In conclusion, we showed that the resonant external modulation of a three-level artificial atom is highly advantageous for the implementation of the antidynamical Casimir effect (ADCE) in comparison to a two-level atom, since the transition rate can suffer almost 50-fold increase while the

total number of annihilated excitations is roughly the same. The strongest gain takes place in the double-resonant regime (when $\Delta_1 = -\Delta_2$, so that $\Omega_{02} = 2\omega_0$) and for large detuning $|\Delta_1|$, though weaker enhancement may occur also in other regimes. Besides speeding up the ADCE, the use of qutrits also loosens the requirements for accurate tuning of the modulation frequency, and reproduces the characteristic ADCE behavior of a qubit when all the atomic transitions are largely detuned from the cavity field (and $\Omega_{02} \neq 2\omega_0$). However, for the optimum annihilation of excitations from a thermal state the usage of qutrits also brings some inconveniences, such as two-tone driving and the necessity of controlling the phase difference between different components of the modulation. Nevertheless, our results indicate that the substantial gain in the transition rate compensates for the additional complexity in the external control, favoring the experimental implementation of ADCE.

## ACKNOWLEDGMENTS

A.V.D. acknowledges partial support from the Brazilian agency Conselho Nacional de Desenvolvimento Científico e Tecnológico (CNPq). B.M. acknowledges financial support from the International Centre for Condensed Matter Physics during his visit to the University of Brasilia.

[1] G. T. Moore, J. Math. Phys. **11**, 2679 (1970).
[2] S. A. Fulling and P. C. W. Davies, Proc. R. Soc. London A **348**, 393 (1976).
[3] C. M. Wilson, G. Johansson, A. Pourkabirian, M. Simoen, J. R. Johansson, T. Duty, F. Nori, and P. Delsing, Nature (London) **479**, 376 (2011).
[4] P. Lähteenmäki, G. S. Paraoanu, J. Hassel, and P. J. Hakonen, Proc. Natl. Acad. Sci. USA **110**, 4234 (2013).
[5] V. V. Dodonov, Phys. Scr. **82**, 038105 (2010).
[6] P. D. Nation, J. R. Johansson, M. P. Blencowe, and F. Nori, Rev. Mod. Phys. **84**, 1 (2012).
[7] S. W. Doescher and M. H. Rice, Am. J. Phys. **37**, 1246 (1969).
[8] V. V. Dodonov, A. B. Klimov, and D. E. Nikonov, J. Math. Phys. **34**, 3391 (1993).
[9] S. Di Martino, F. Anza, P. Facchi, A. Kossakowski, G. Marmo, A. Messina, B. Militello, and S. Pascazio, J. Phys. A **46**, 365301 (2013).
[10] C. K. Law, Phys. Rev. A **49**, 433 (1994).
[11] A. Lambrecht, M.-T. Jaekel, and S. Reynaud, Phys. Rev. Lett. **77**, 615 (1996).
[12] T. Fujii, S. Matsuo, N. Hatakenaka, S. Kurihara, and A. Zeilinger, Phys. Rev. B **84**, 174521 (2011).
[13] V. V. Dodonov, Phys. Lett. A **207**, 126 (1995).
[14] N. B. Narozhny, A. M. Fedotov, and Y. E. Lozovik, Phys. Rev. A **64**, 053807 (2001).
[15] A. V. Dodonov, R. L. Nardo, R. Migliore, A. Messina, and V. V. Dodonov, J. Phys. B **44**, 225502 (2011).
[16] A. V. Dodonov and V. V. Dodonov, Phys. Lett. A **375**, 4261 (2011).
[17] A. V. Dodonov and V. V. Dodonov, Phys. Rev. A **85**, 015805 (2012).
[18] A. V. Dodonov and V. V. Dodonov, Phys. Rev. A **85**, 063804 (2012).
[19] A. S. M. de Castro, A. Cacheffo, and V. V. Dodonov, Phys. Rev. A **87**, 033809 (2013).
[20] A. V. Dodonov, Phys. Scr. **87**, 038103 (2013).
[21] A. V. Dodonov and V. V. Dodonov, Phys. Rev. A **85**, 055805 (2012).
[22] A. V. Dodonov and V. V. Dodonov, Phys. Rev. A **86**, 015801 (2012).
[23] S. Felicetti, M. Sanz, L. Lamata, G. Romero, G. Johansson, P. Delsing, and E. Solano, Phys. Rev. Lett. **113**, 093602 (2014).
[24] R. Stassi, S. De Liberato, L. Garziano, B. Spagnolo, and S. Savasta, Phys. Rev. A **92**, 013830 (2015).
[25] D. Z. Rossatto, S. Felicetti, H. Eneriz, E. Rico, M. Sanz, and E. Solano, Phys. Rev. B **93**, 094514 (2016).
[26] A. V. Dodonov, J. Phys.: Conf. Ser. **161**, 012029 (2009).
[27] S. De Liberato, D. Gerace, I. Carusotto, and C. Ciuti, Phys. Rev. A **80**, 053810 (2009).
[28] F. Beaudoin, J. M. Gambetta, and A. Blais, Phys. Rev. A **84**, 043832 (2011).
[29] F. Beaudoin, M. P. da Silva, Z. Dutton, and A. Blais, Phys. Rev. A **86**, 022305 (2012).
[30] G. Vacanti, S. Pugnetti, N. Didier, M. Paternostro, G. M. Palma, R. Fazio, and V. Vedral, Phys. Rev. Lett. **108**, 093603 (2012).
[31] A. V. Dodonov, J. Phys. A **47**, 285303 (2013).
[32] J. D. Strand, M. Ware, F. Beaudoin, T. A. Ohki, B. R. Johnson, A. Blais, and B. L. T. Plourde, Phys. Rev. B **87**, 220505(R) (2013).
[33] G. Benenti, A. D'Arrigo, S. Siccardi, and G. Strini, Phys. Rev. A **90**, 052313 (2014).
[34] I. M. de Sousa and A. V. Dodonov, J. Phys. A **48**, 245302 (2015).
[35] A. V. Dodonov, B. Militello, A. Napoli, and A. Messina, Phys. Rev. A **93**, 052505 (2016).
[36] X. Gu, A. F. Kockum, A. Miranowicz, Y.-X. Liu, and F. Nori, arXiv:1707.02046.
[37] A. Blais, R.-S. Huang, A. Wallraff, S. M. Girvin, and R. J. Schoelkopf, Phys. Rev. A **69**, 062320 (2004).
[38] A. Wallraff, D. I. Schuster, A. Blais, L. Frunzio, R.-S. Huang, J. Majer, S. Kumar, S. M. Girvin, and R. J. Schoelkopf, Nature (London) **431**, 162 (2004).
[39] J. Koch, T. M. Yu, J. Gambetta, A. A. Houck, D. I. Schuster, J. Majer, A. Blais, M. H. Devoret, S. M. Girvin, and R. J. Schoelkopf, Phys. Rev. A **76**, 042319 (2007).
[40] J. Q. You and F. Nori, Nature (London) **474**, 589 (2011).
[41] C. Axline *et al.*, Appl. Phys. Lett. **109**, 042601 (2016).
[42] J. Majer *et al.*, Nature (London) **449**, 443 (2007).
[43] M. Hofheinz *et al.*, Nature (London) **459**, 546 (2009).
[44] L. DiCarlo *et al.*, Nature (London) **460**, 240 (2009).
[45] M. S. Allman, F. Altomare, J. D. Whittaker, K. Cicak, D. Li, A. Sirois, J. Strong, J. D. Teufel, and R. W. Simmonds, Phys. Rev. Lett. **104**, 177004 (2010).
[46] A. J. Hoffman, S. J. Srinivasan, J. M. Gambetta, and A. A. Houck, Phys. Rev. B **84**, 184515 (2011).

[47] J. M. Gambetta, A. A. Houck, and A. Blais, Phys. Rev. Lett. **106**, 030502 (2011).
[48] H. Paik, D. I. Schuster, L. S. Bishop, G. Kirchmair, G. Catelani, A. P. Sears, B. R. Johnson, M. J. Reagor, L. Frunzio, L. I. Glazman, S. M. Girvin, M. H. Devoret, and R. J. Schoelkopf, Phys. Rev. Lett. **107**, 240501 (2011).
[49] T. Niemczyk, F. Deppe, H. Huebl, E. P. Menzel, F. Hocke, M. J. Schwarz, J. J. Garcia-Ripoll, D. Zueco, T. Hummer, E. Solano, A. Marx, and R. Gross, Nat. Phys. **6**, 772 (2010).
[50] J. Casanova, G. Romero, I. Lizuain, J. J. García-Ripoll, and E. Solano, Phys. Rev. Lett. **105**, 263603 (2010).
[51] A. Baust, E. Hoffmann, M. Haeberlein, M. J. Schwarz, P. Eder, J. Goetz, F. Wulschner, E. Xie, L. Zhong, F. Quijandria, D. Zueco, J.-J. G. Ripoll, L. Garcia-Alvarez, G. Romero, E. Solano, K. G. Fedorov, E. P. Menzel, F. Deppe, A. Marx, and R. Gross, Phys. Rev. B **93**, 214501 (2016).
[52] P. Forn-Díaz, J. J. García-Ripoll, B. Peropadre, J.-L. Orgiazzi, M. A. Yurtalan, R. Belyansky, C. M. Wilson, and A. Lupascu, Nat. Phys. **13**, 39 (2017).
[53] C. Navarrete-Benlloch, J. J. García-Ripoll, and D. Porras, Phys. Rev. Lett. **113**, 193601 (2014).
[54] D. S. Veloso and A. V. Dodonov, J. Phys. B **48**, 165503 (2015).
[55] A. V. Dodonov, D. Valente, and T. Werlang, Phys. Rev. A **96**, 012501 (2017).
[56] F. Hoeb, F. Angaroni, J. Zoller, T. Calarco, G. Strini, S. Montangero, and G. Benenti, arXiv:1706.00048.
[57] I. I. Rabi, Phys. Rev. **49**, 324 (1936).
[58] I. I. Rabi, Phys. Rev. **51**, 652 (1937).
[59] D. Braak, Phys. Rev. Lett. **107**, 100401 (2011).
[60] L. C. Monteiro and A. V. Dodonov, Phys. Lett. A **380**, 1542 (2016).
[61] E. L. S. Silva and A. V. Dodonov, J. Phys. A **49**, 495304 (2016).
[62] See Supplemental Material at http://link.aps.org/supplemental/10.1103/PhysRevA.96.032509 for the detailed analysis of the population differences and the ADCE transition rates.